A pH-responsive polyelectrolyte multilayer film with tunable interfacial properties

Jiang, Tao; Moghaddam, Saeed Zajforoushan; Thormann, Esben

Published in:
Polymer

Link to article, DOI:
10.1016/j.polymer.2020.123367

Publication date:
2021

Document Version
Peer reviewed version

A pH-responsive Polyelectrolyte Multilayer Film with Tunable Interfacial Properties

Tao Jiang, Saeed Zajforoushan Moghaddam, Esben Thormann*

Department of Chemistry, Technical University of Denmark, 2800 Kgs. Lyngby, Denmark

Corresponding author: esth@kemi.dtu.dk, +45 45 25 24 39

Abstract. We report a facile and versatile approach to fabricate polyelectrolyte multilayer (PEM) films with a chemically modifiable outer surface. A PEM film was prepared by layer-by-layer assembly of poly (2-aminoethyl methacrylate) (PAMA) and polymethacrylic acid (PMAA), terminated with a partially tert-butyloxycarbonyl (Boc)-protected random copolymer (PAMA-co-PBocAMA) as the final layer. The obtained PEM film was then cross-linked and the free amino groups in the PEM film were quenched using EDC/NHS chemistry. The outer layer of the film was then treated via a deprotection reaction, affording free amino groups selectively located at the film surface. As a proof of concept study, these functional groups were used to modify the film surface with two model hydrophilic and hydrophobic compounds, which tuned the wettability of the PEM.

Keywords: Polyelectrolyte multilayer, surface modification, EDC/NHS cross-linking, pH-responsive film

1. Introduction

Polymeric thin-films allow diverse surface modification possibilities to fabricate surfaces with controlled interfacial properties.[1–4] Different methods are available to prepare polymer-coated surfaces,[5–9] among which the layer-by-layer (LbL) assembly is regarded as a facile and versatile method.[10–13] In a typical LbL process, two oppositely charged polyelectrolytes are alternately deposited onto a charged substrate, producing a polyelectrolyte multilayer (PEM) film. Such polymeric coatings can possess distinguished physicochemical properties and functionality within (bulk properties) and at the surface (interfacial properties). Examples of bulk properties include film viscoelasticity,[14,15] hydration,[16] conductivity,[17], and permeability.[18] The interfacial properties include surface wettability and adhesion [19,20] as well as selective adsorption.[21] It is of interest, from both fundamental and applied points of view, to develop PEM films where the interfacial properties can be tuned systematically.

In the literature, several approaches have been developed to selectively tune the interfacial properties of PEM films. In one approach, the LBL process is terminated with a functional layer that provides a desired interfacial functionality.[22–25] As an example, Easton et al. fabricated poly(acrylic acid)/polyethyleneimine PEM coatings terminated with an active heparin layer, which promoted proliferation and migration of vascular endothelial cells.[26] In another study, Chang et al. deposited heparin as the final layer on a poly(acrylic acid)/chitosan PEM film, which efficiently reduced the cell adhesion to a silicone rubber substrate.[27] Another approach to modify the PEM interfacial properties is via post-assembly modification of the outer layer through chemical functionalization. For instance, Delgado et al. capped a poly(styrene sulfonate)/poly(diallyldimethylammonium chloride) PEM film with

a co-polymer containing benzyl mercaptan units to introduce thiol groups selectively in the outer layer.[21] The chemical reactivity of the thiol groups was utilized to bind various functional components, e.g., the Arg-Gly-Asp (RGD) adhesive peptide for enhanced cell adhesion, poly(ethylene glycol) units for reduced biofouling, and gold nanoparticles.

Adopting a combination of these two approaches, we hereby demonstrate a versatile method to prepare PEM films with chemically tunable outer layers. To do so, a PEM film comprising poly (2-amino)ethyl methacrylate (PAMA) and polymethacrylic acid (PMAA) was first prepared by LbL assembly. Afterward, a partially protected PAMA-*co*-PBocAMA random copolymer was deposited as the outer layer of the film. The film was then stabilized by chemical cross-linking catalyzed by EDC/NHS, followed by quenching the remaining amino groups in the film. This step minimizes the number of remaining amino groups in the bulk film so that the later chemical coupling of the amine groups has little effect on the chemical composition in the bulk film. Finally, the Boc groups in the outer layer were removed in trifluoroacetic acid, giving rise to a cross-linked PEM film with reactive amino groups selectively in the outer layer. The interfacial properties of the obtained PEM film can be modified by an amidation reaction using carboxylic acid derivatives with desired functionalities. As a proof of concept, two carboxylic acid derivatives with comparable chain lengths yet different hydrophilicity, i.e., m-PEG3-COOH and undecanoic acid, were coupled to the PEM, and different contact angles of the modified films were observed confirming the successful outer layer modification.

2. Experimental Section

2.1 Materials

(2-Boc-amino)ethyl methacrylate (BocAMA, 99%), tert-Butyl methacrylate (tBuMA, 98%,

passed through neutral alumina column to remove inhibitor immediately before use), ethyl α-bromoisobutyrate (EBiB, 98%), trifluoroacetic acid (TFA, 99%), (3-aminopropyl)triethoxysilane (APTES, 99%), N,N,N′,N′′,N′′-pentamethyldiethylenetriamine (PMDETA, 99%), copper(I) chloride (CuCl, >99%, washed sequentially with acetic acid and ethanol before use), N-(3-dimethylaminopropyl)-N′-ethylcarbodiimide hydrochloride (EDC, 99%), N,N'-Dicyclohexylcarbodiimide (DCC, 99%), N-hydroxysuccinimide (NHS, >98%), and undecanoic acid (99%) were all purchased from Sigma Aldrich and used as received unless otherwise stated. m-PEG3-COOH (98%) was purchased from BroadPharm (USA) and used as received. All the solvents used in this work were of HPLC grade from Sigma Aldrich. All the solutions were prepared with ultra-pure water (Sartorius Arium® pro ultrapure water system, resistivity of 18.2 MΩ cm). Citric acid (>99.5%), sodium phosphate monobasic dihydrate (99%), and sodium phosphate dibasic dihydrate (99%) were purchased from Sigma Aldrich and used as received for buffer preparation. To prepare the pH 4.4 citric acid/phosphate buffer (used for LbL assembly), 1.074 g of citric acid and 1.57 g of $Na_2HPO_4 \bullet 2H_2O$ were used to prepare a 100 ml solution with a volumetric flask. Phosphate buffers used in cross-linking and pH cycles were prepared by adjusting the pH of a 50 mM NaH_2PO_4 solution with either 1M HCl or NaOH. All the buffers were vacuum-filtered with a Millipore 0.1 µm regenerated cellulose membrane and degassed under vacuum immediately before use. All the polymer solutions used were filtered with a 0.22 µm nylon syringe filter and degassed under vacuum before use.

2.2 Synthesis of PAMA, PMAA, and PAMA-*co*-PBocAMA

Poly(2-aminoethyl methacrylate) (PAMA) and poly(methacrylic acid) (PMAA) were synthesized by atom transfer radical polymerization (ATRP).[28,29] To avoid deactivation of the Cu catalyst by the carboxyl and amino groups, a two-step protection-deprotection

procedure was adopted. The protected PBocAMA and PtBMAA were first synthesized and further deprotected under acidic condition (TFA/DCM) to yield the desired PAMA and PMAA polymers. In addition, the PBocAMA polymer underwent a short-time deprotection process (10 min) to yield the partially protected PAMA-*co*-PtBocAMA copolymer. Scheme 1 summarizes the chemical structures of the used reagents as well as the synthesized polyelectrolytes. The three polyelectrolytes obtained were characterized by ^{1}H NMR and AF4. The average molecular weights and the polydispersity indices (PDI) are presented in Table 1. Detailed synthesis procedures and characterizations are provided in the supporting information (Section S1).

Table 1 *Characterization data of the synthesized polymers*

	Mn[1] (kDa)	***Mn[2] (kDa)***	***PDI[2]***	***BocAMA content (DP%)***
PAMA	11.9	11.1	1.26	-
PMAA	6.1	6.5	1.49	-
PAMA-*co*-PBocAMA	17.7	16.5	1.26	63%

[1] Determined with ^{1}H NMR; [2] Determined with AF4

2.3 Preparation of the PMAA/PAMA PEM film with a chemically modifiable outer layer

The LbL assembly of the PEM was conducted on silica-coated QCM-D sensors (QSX 335, Biolin Scientific) in the standard module for simultaneous QCM-D and ellipsometry measurements (QELM 401, Biolin Scientific, Gothenburg, Sweden). The sensor was aminated with APTES before use.[30] For that, the sensor was rinsed with copious amounts of ethanol and water, dried with compressed air, followed by a plasma treatment for 1 min (PDC-32G plasma cleaner, Harrick Plasma) in water vapor under a constant pressure of 0.5 Torr. Afterward, the sensor was placed in a vacuumed desiccator with a 50% (v/v) APTES/toluene solution for 18 h. After rinsing with copious amounts of toluene and ethanol and drying, the sensor was mounted into the QCM-D module and the measurement was started at 23 °C. The citric

acid/phosphate buffer at pH 4.4 was loaded using a 75 µL/min flow rate. After reaching a stable baseline, PMAA and PAMA solutions (100 ppm) were alternately loaded (15min) having rinsing steps (10 min) with the buffer in between. Finally, PAMA-*co*-PBocAMA was deposited as the last layer (14th layer) using the same procedure. After LbL assembly, the PEM film was cross-linked by loading a 5 mg/ml EDC/NHS solution into the module for 2h. To test the pH stability, pH 2.5, 4.5, and 9 solutions (50 mM NaH_2PO_4 solution, pH adjusted using 1M NaOH and HCl) were loaded. Three successive pH cycles were conducted between pH 4.5 and 2.5 as well as 4.5 and 9. Afterward, the amino groups in the PEM film were quenched following a similar protocol that we utilized in our previous study.[31] To do so, a solution of 5 mg/ml EDC/NHS, 5 µl/ml acetic acid was loaded into the cell repeatedly for a total of 4 times (2h × 2, plus 12h × 2). The pH-responsiveness was tested after each quenching step to test the quenching efficiency.

To remove the Boc protected groups on the outer layer, the sensor was removed from the QCM-D module, rinsed with water, dried, and immersed in a solution containing 0.5 ml TFA and 4 ml DCM, followed by rinsing with copious ethanol and drying with compressed air.

2.4 Surface modification with undecanoic acid and m-PEG3-COOH

The outer layer of the PEM was modified with either the hydrophobic undecanoic acid or the hydrophilic m-PEG3-COOH. To do so, undecanoic acid (186 mg, 1 mmol) or m-PEG3-COOH (192 mg, 1 mmol) was first dissolved in 2 ml dichloromethane. The solution was then added dropwise under stirring, into a solution of DCC (309 mg, 1.5 mmol) in dichloromethane (3 ml). The reaction mixture was stirred for an extra 5 min before the sensor with the PEM film was

immersed for 12h. After the modification, the sensor was removed from the solution, washed thoroughly with ethanol, and dried with compressed air.

2.5 Methods

2.5.1 In-situ QCM-D and Spectroscopic Ellipsometry

Simultaneous QCM-D and spectroscopic ellipsometry measurements were conducted using the QSense ellipsometry module (QELM 401, Biolin Scientific, Gothenburg, Sweden). For the QCM-D experiment, the shift in the resonance frequency (F) and dissipation factor (D) were recorded. The instrument software (Dfind, Biolin Scientific) was employed for data analysis. Both Sauerbrey[32] and Voigt[33] models were employed for estimation of the film thickness. The Sauerbrey model assumes a simple linear correlation between the adsorbed mass and the frequency shift, which is exclusive to thin and rigid films. Contrarily, the Voigt model can provide a more accurate estimation of the adsorbed mass of hydrated and viscoelastic films. An estimated film density of 1200 $kg \cdot m^{-3}$ was used. The density and viscosity of water at 23 °C (from the software library) was used for the medium.

A spectroscopic ellipsometer (M-2000U, JA Woollam Co., USA) was used in combination with QCM-D. Spectroscopic Ψ (amplitude ratio) and Δ (phase shift) were collected (wavelength range: 245 - 1000 nm, angle of incidence of 70°). The instrument software (CompleteEASE, JA Woollam Co., USA) was used for data modeling. The bare sensor was first modeled as a pseudosubstrate consisting of a silica coating (25 nm, tabulated optical constants) and a thick, optically opaque titanium substrate. The optical constants of the Ti substrate were modeled using a B-Spline model (resolution 0.2 eV, tabulated Ti optical constants used as the initial estimate values). The fitted parameters for the substrate were then fixed in the model. The PEM film was regarded as a transparent and homogeneous layer with no light absorption

(k=0); then, the film thickness and the refractive index (n) were estimated using the Cauchy equation.[34] To estimate the water content, the film was modeled as a two-component layer consisting of dry polymer (A = 1.5 and B = 0.005),[35,36] and water with tabulated optical constants. The volume fraction of water (f_w) was then estimated according to the Bruggeman Effective Medium Approximation (BEMA).[37]

2.5.2 Contact angle measurement

The water contact angle (Attension Theta Lite tensiometer, Biolin Scientific) on the PEM films was measured in the air using the sessile drop method at ambient temperature. A water droplet with the volume of 1 µL was placed by a Hamilton syringe onto the sample surface, and the contact angle value after 5 seconds was then determined using the Young−Laplace equation. A mean value of the left and right contact angles of three measurements is reported herein.

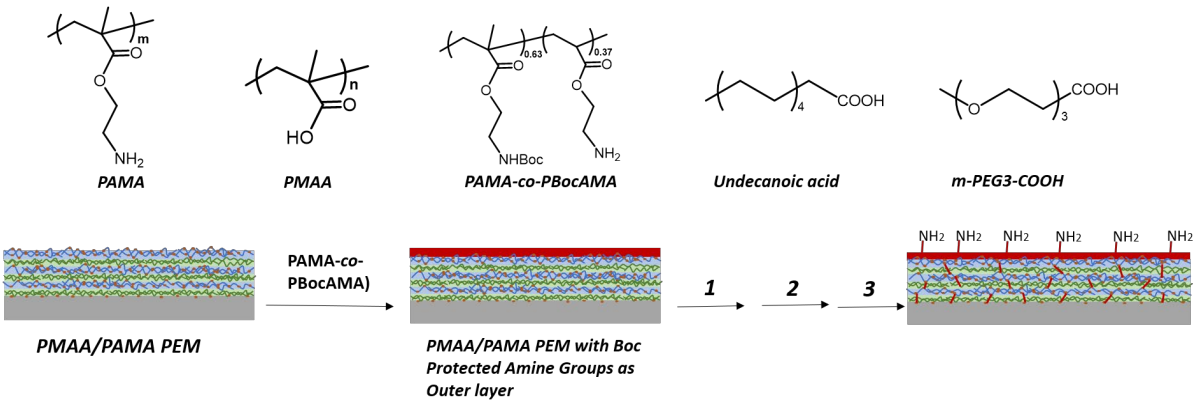

Scheme 1 *Chemical structures of the synthesized polyelectrolytes and the used reagents, as well as the illustration of the fabrication of the PMAA/PAMA PEM film with the chemically modifiable outer layer*

3 Results and Discussion

3.1 LbL assembly of PAMA/PMAA

Figure 1a presents the QCM-D shifts in the resonance frequency (F) and dissipation factor (D) for the 3rd overtone, resulting from the LbL assembly of the PMAA/PAMA film. The odd and even layer numbers refer to the deposition of PMAA and PAMA layers, respectively, while the final layer (layer 14) denotes the deposition of the PAMA-*co*-PBocAMA copolymer. The decrease in frequency and increase in dissipation indicate continuous mass deposition on the substrate. The overall shifts in frequency and dissipation for seven bilayers are approximately -220 Hz and 1×10^{-6}, respectively. This provides a notably small $\Delta D/\Delta F$ ratio of around 0.0045 $\times 10^{-6}$ Hz^{-1}, which suggests a highly rigid film structure with low water content.[38] Notably, the deposition of PAMA-*co*-PBocAMA (last layer) shows a relatively larger dissipation shift compared to those of PAMA depositions. This observation suggests that the outermost PAMA-*co*-PBocAMA layer adopts a more coil-like and less rigid conformation compared to the PAMA layers, which may be attributed to the relatively lower charge density (~ 60% protected uncharged groups) of PAMA-*co*-PBocAMA. The film thickness was estimated using both Sauerbrey and viscoelastic Voigt models (Figure 1b). A close match between both models is found, which further confirms the rigid nature of the film.[38] The acoustic thickness (i.e., measured by QCM-D) of the film (14 layers) is then estimated to be around 35 nm. In addition, the thickness versus the number of layers demonstrates a closely linear trend (~ 5 nm per each bilayer). As reported in the literature, a linear growth mechanism is observed when the deposited polyelectrolytes cannot freely diffuse through the film, which seems to be the case herein.[39–41] Hence, we can assume that the deposited PAMA-*co*-PBocAMA has limited freedom to diffuse within the film and is immobilized at the film surface. Such a property is

important for our work, which requires the modifiable amino groups predominantly in the outer layer of the PEM film.

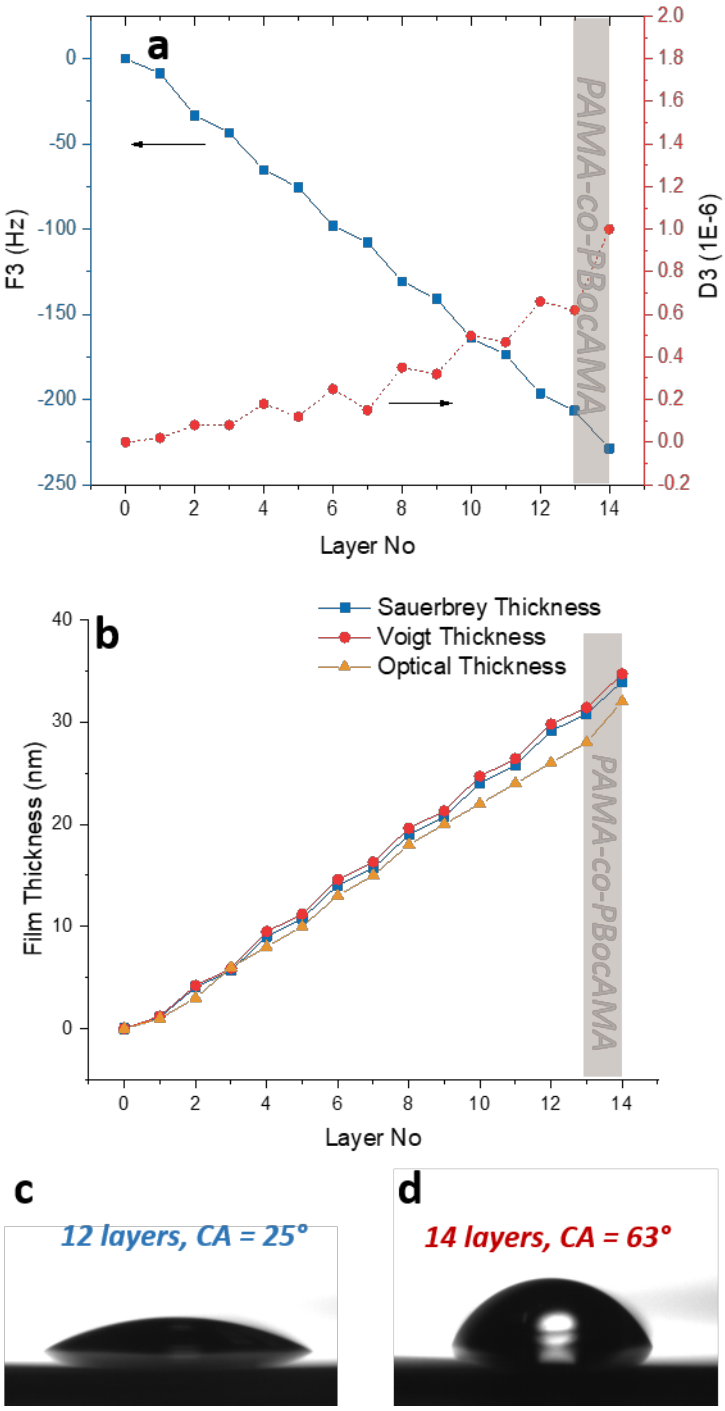

Figure 1 *LbL assembly of PAMA and PMAA, with PAMA-co-PBocAMA as the final layer in pH 4.4 citric acid/phosphate buffer: a) Frequency and dissipation shifts throughout the LbL process, with odd layers of PMAA and even layers of PAMA (PAMA-co-BocAMA as the final layer), b) Film thickness as a function of layer number from QCM-D (Sauerbrey and Voigt thicknesses) and spectroscopic ellipsometry (optical*

thickness), c) Contact angle measured on PEM with 12 layers (PAMA as the final layer), d) Contact angle measured on PEM with 14 layers (PBocAMA as the final layer)

The layer growth was simultaneously monitored with spectroscopic ellipsometry. The estimated optical thickness of the film from the ellipsometry measurement is around 31 nm (Figure 1b), which is relatively similar to the estimated acoustic thickness from QCM-D. The slightly larger acoustic thickness can be attributed to different measurement principles and detection limits of the investigation methods, i.e., ellipsometry is more sensitive to the dense bulk-like part of the film, whereas QCM-D is sensitive to the slipping plane. The water content of the film is estimated (using BEMA) to be around 20 v/v%. The relatively low water content of the film is in agreement with the notably small QCM-D dissipation shift. Such a compact structure of the PEM film can be attributed to a relatively high charge density of the polyelectrolytes and consequently a strong complexation between the PMAA and PAMA polymer chains.

To further test the difference between a fully deprotected PAMA and partially protected PAMA-*co*-PBocAMA final layer, the contact angle of the film was measured when having PAMA (12 layers, Figure 1c) or PAMA-*co*-PBocAMA as the outer layer (14 layers, Figure 1d). A clear variation in water contact angle between layer 12 (25 ± 1°) and layer 14 (63 ± 2°) is observed, which can be attributed to the relatively low charge density of PAMA-*co*-PBocAMA and the high hydrophobicity of the Boc protected groups.

3.2 Cross-linking and quenching of amino groups by EDC/NHS coupling

PEM films comprising weak polyelectrolytes are prone to disintegration upon pH variations, which originates from the charge imbalance within the film. To stabilize the PEM film prepared herein, the amino groups and the carboxyl groups in the film were cross-linked using

EDC/NHS coupling chemistry.[42] Next, a pH cycle experiment was performed to examine the pH stability of the film. Figure 2 presents the QCM-D frequency and dissipation shifts (panel a), as well as the estimated optical thickness/water content (panel b) of the film following the pH cycles. Decreasing the pH from 4.5 to 2.5 results in an increment in dissipation and decrement in frequency, which together imply swelling of the film. Similarly, the estimated optical thickness roughly increases from 31 nm to 52 nm together with a gain in the water content from 20 % to 50%. Increasing the pH back to 4.5 results in the film collapse yet with a moderate degree of structural hysteresis. Nevertheless, the subsequent pH cycles exhibit a nearly reversible swelling-shrinking process with minor hysteresis, indicating enhanced stability of the cross-linked film under the acidic condition. The subsequent pH cycles between 4.5 to 9 also demonstrate reversible swelling/shrinkage of the film under the alkaline condition.

The swollen film conformation at pH 2.5 can be attributed to the net positive charge of the film, which originates from the protonation of the excess amino groups. The unreacted amino groups within the bulk film are not desirable for our work, because we aim to prepare a film with amino groups chiefly in the outermost layer. Therefore, a formerly described amine quenching process was conducted to effectively reduce the amine content in the film interior.[31] To do so, a solution of EDC/NHS, together with acetic acid, was flowed over the surface repeatedly for four consecutive cycles. Herein, acetic acid will bind to the amino groups within the film turning them into amide groups that are no longer reactive towards the later modification.

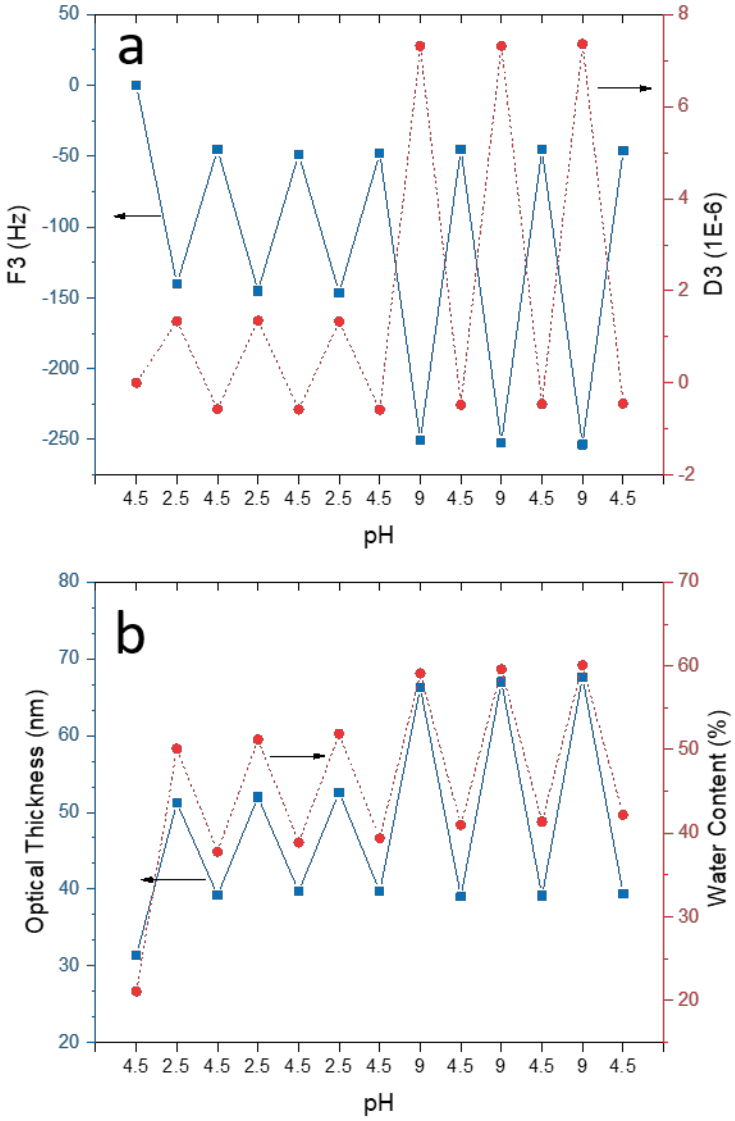

Figure 2 *pH-responsiveness of the film after cross-linking with EDC/NHS: a) QCM-D Frequency and dissipation and b) Optical thickness and water content (obtained from ellipsometry) following the pH cycles between pH 4.5 and 2, pH 4.5 and 9.*

We examined the pH-responsiveness of the film under the acidic condition (after each quenching cycle) to test the efficiency of the amine elimination process. As shown in the supporting information (Figure S5), the frequency and dissipation shifts associated with changing the pH from 4.5 to 2.5 both decrease in magnitude during the quenching process, indicating a subsequent decrease in the amine content. Figure 3 shows the pH-responsiveness of the cross-linked PEM film after the amine quenching process. Regarding the pH cycles

between 4.5 and 2.5, it is evident that the shifts in QCM-D frequency, as well as in the optical thickness and water content of the film, are significantly attenuated. This indicates that the population of the amino groups, which can produce film swelling under acidic conditions, is decreased. Notably, while the optical thickness shows very little pH-dependence, the QCM-D data (in particular the dissipation data) indicates some degree of responsiveness to the acidic condition, which can be attributed to the structural changes mainly at the film surface. In contrast, the amine quenching has a minor effect on the pH-responsiveness of the film under alkaline conditions, i.e., the swelling behavior before and after the amine quenching is similar.

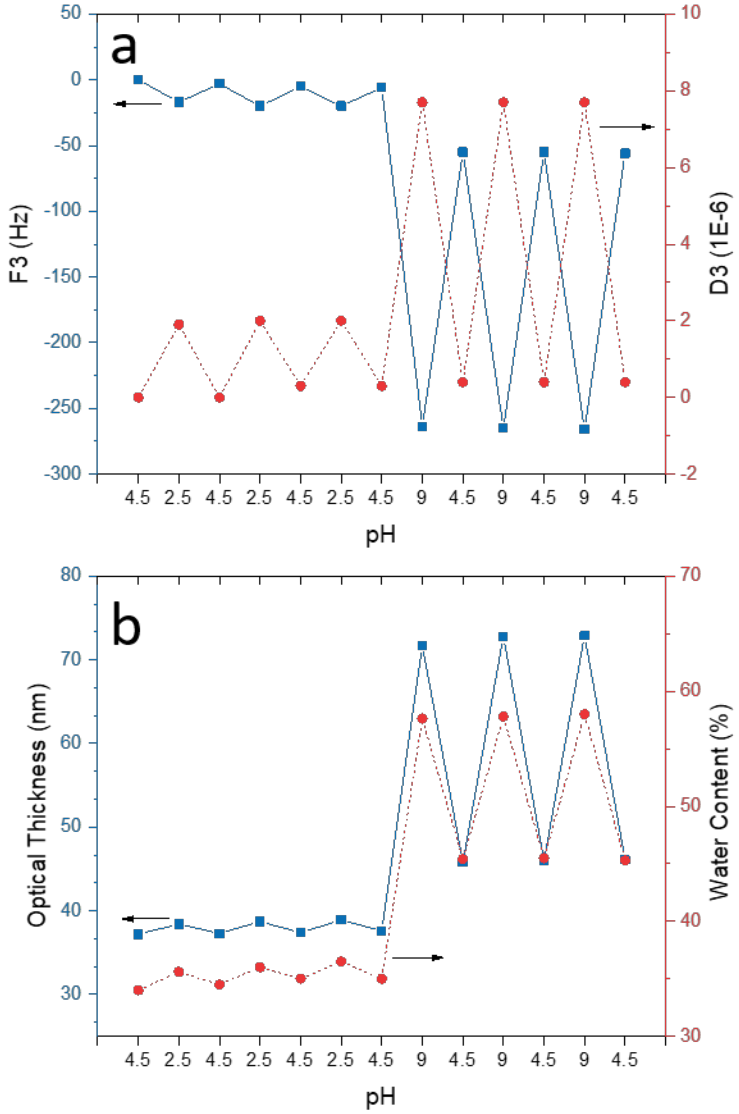

Figure 3 *pH-responsiveness of the film after amine quenching: a) QCM-D Frequency and dissipation and b) Optical thickness and water content (obtained from ellipsometry) following the pH oscillation test between pH 4.5 and 2, pH 4.5 and 9*

3.3 Surface deprotection and modification of PMAA/PAMA PEM film

Next, we discuss how deprotection of the Boc-protected amino groups can modify the outermost PAMA-*co*-PBocAMA layer. Figure 4 presents the contact angles of the PEM film as a function of the duration of TFA/DCM treatment. The initial contact angle of the film (before deprotection) was around 60 ± 3°. Following the deprotection process, a decrement in the contact angle was observed, which can be attributed to the transform of the hydrophobic Boc

groups to the hydrophilic amino groups on the surface. The contact angle value reaches a plateau of around 37 ± 2° roughly after 60 min of TFA/DCM treatment, which suggests a major removal of the Boc protection groups. The unprotected amino groups at the film surface will allow post-modification of the interfacial properties. Here, we selected two model carboxylic acid derivatives with similar chain lengths, one hydrophilic (m-PEG3-COOH) and the other hydrophobic (undecanoic acid), to modify the wetting properties of the film as a proof of concept. Figure 5 compares the contact angles of the modified PEM films. Modification with m-PEG3-COOH led to a contact angle of 55 ± 2°, which is in accordance with the typical literature value of a surface modified by PEG units.[43,44] Contrarily, modification of the film surface with undecanoic acid resulted in an increment in the contact angle from 37 ± 2° to 78 ± 3°. Despite a relatively high contact angle of 78 ± 3°, it should be noted that the surface cannot be regarded as hydrophobic. We speculate the reason to be a relatively low density of the amine groups that are accessible for surface grafting, which may be improved by using a PAMA-*co*-PBocAMA copolymer with a higher degree of protected groups.

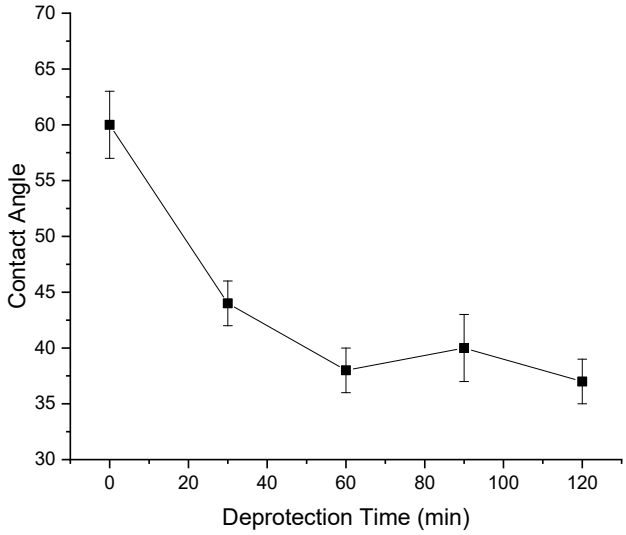

Figure 4 *Contact angle measured along the deprotection process, with a time interval of 30 min*

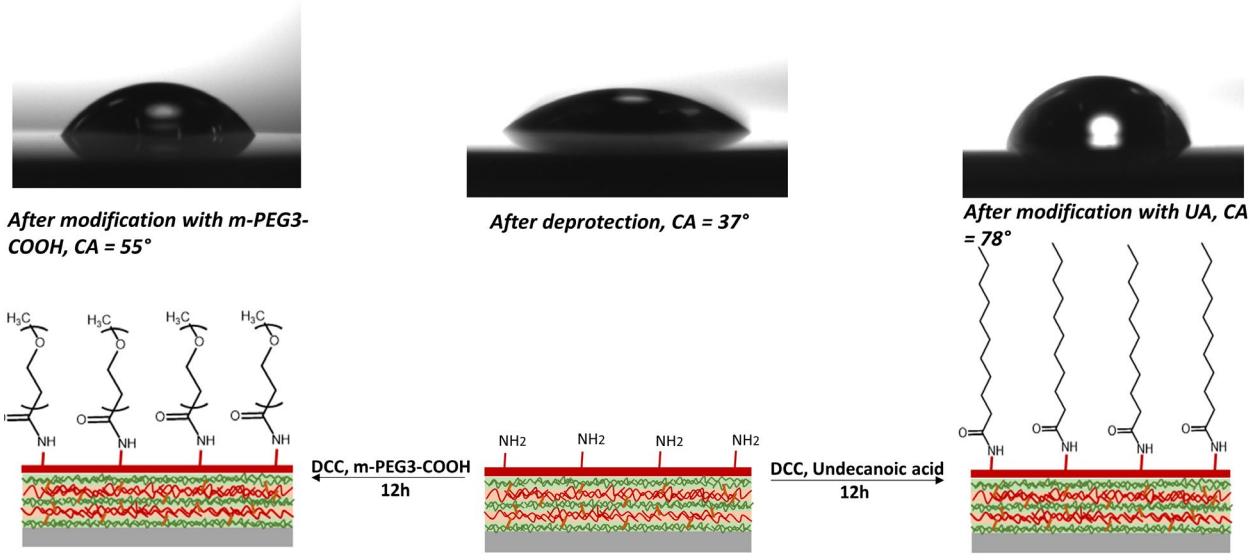

Figure 5 *Contact angles measured before and after surface modification with undecanoic acid and m-PEG3-COOH with DCC as cross-linking agent*

We also tested the pH-responsive behavior of the surface-modified PEM films to check if the surface modification process affects the pH-responsiveness of the film. Figure 6 demonstrates the QCM-D frequency and dissipation shifts resulting from the pH cycles. The observed pH-responsive pattern is similar to that of after amine quenching, indicating a minimum effect of

the surface modification on the pH-responsiveness of the film and bulk properties. Therefore, the method demonstrated herein can be a versatile approach to the preparation of cross-linked and pH-responsive PEM films with tunable interfacial properties.

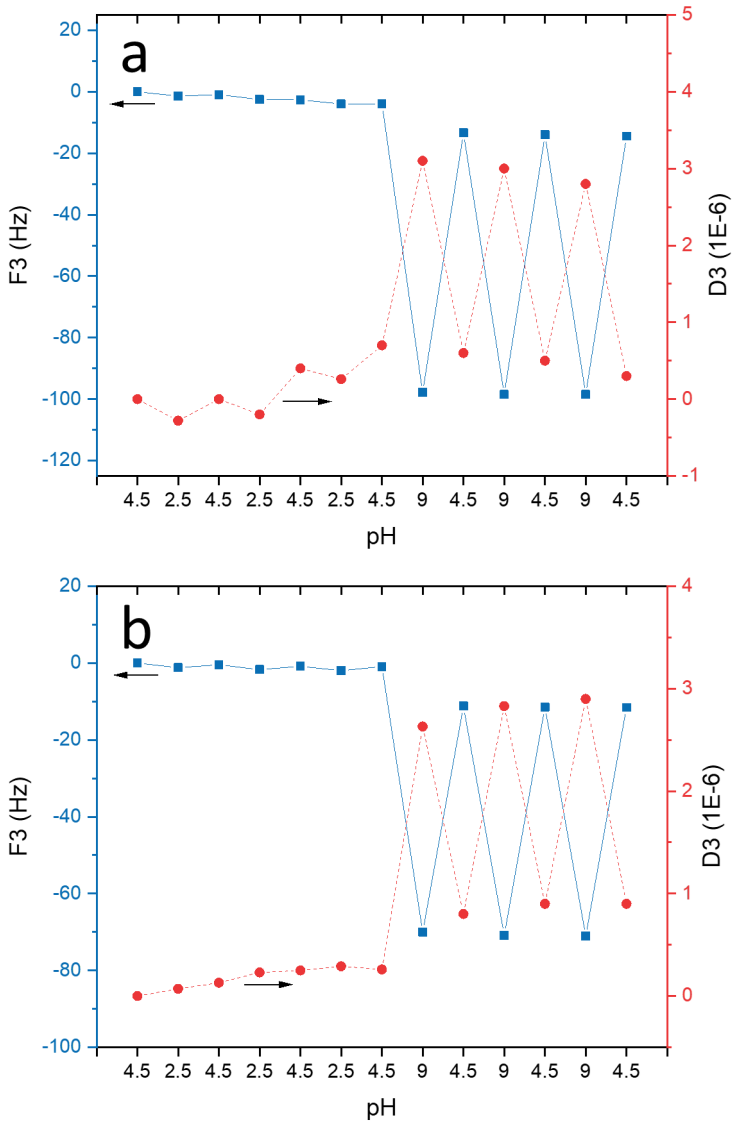

Figure 6 *Frequency and dissipation shifts corresponding to a pH cycle from pH 4.5 to pH 2.5, and pH 4.5 to pH 9, after surface modification with a) undecanoic acid, b) m-PEG3-COOH*

Conclusion

We demonstrated a simple and versatile approach to fabricate a pH-responsive PEM film with a chemically modifiable outer layer. The QCM-D and ellipsometry data indicated that the

prepared PMAA/PAMA multilayer film shows pH-responsiveness due to the amine and carboxyl groups present in the film. We quenched the amino groups inside the film and removed the Boc protection groups on the outer layer. As a result, a PEM film was obtained that comprised primary amino groups selectively in the outer layer, allowing chemical modification of the film surface using carbodiimide chemistry. As proof of concept, the film outer layer was modified with m-PEG3-COOH and undecanoic acid. The PEGylated surface showed a contact angle of approximately 55 ± 2°, while the surface modified with undecanoic acid exhibited relatively higher hydrophobicity with a contact angle of 78 ± 3°. Moreover, a similar pH-responsiveness of the two modified PEM films was observed, suggesting a minimum effect of the surface modification on the bulk property of the film. This work thus described a new procedure in fine-tuning the interfacial property of a PEM film for a wide range of applications.

Acknowledgment

T. J. and E. T. would like to acknowledge the financial support from the Independent Research Fund Denmark (grant # 6111-00102B).

References

[1] D. Rana, T. Matsuura, Surface Modifications for Antifouling Membranes, Chem. Rev. 110 (2010) 2448–2471. https://doi.org/10.1021/cr800208y.

[2] A. Erdemir, Review of engineered tribological interfaces for improved boundary lubrication, Tribol. Int. 38 (2005) 249–256. https://doi.org/10.1016/j.triboint.2004.08.008.

[3] M.J. Kreder, J. Alvarenga, P. Kim, J. Aizenberg, Design of anti-icing surfaces: smooth, textured or slippery?, Nat. Rev. Mater. 1 (2016) 15003. https://doi.org/10.1038/natrevmats.2015.3.

[4] A.C. Duncan, F. Weisbuch, F. Rouais, S. Lazare, C. Baquey, Laser microfabricated model surfaces for controlled cell growth, Biosens. Bioelectron. 17 (2002) 413–426. https://doi.org/10.1016/S0956-5663(01)00281-0.

[5] P.K. Chu, J.Y. Chen, L.P. Wang, N. Huang, Plasma-surface modification of biomaterials, Mater. Sci. Eng. R Reports. 36 (2002) 143–206. https://doi.org/10.1016/S0927-796X(02)00004-9.

[6] J.J. Gooding, F. Mearns, W. Yang, J. Liu, Self-Assembled Monolayers into the 21st Century: Recent

Advances and Applications, Electroanalysis. 15 (2003) 81–96. https://doi.org/10.1002/elan.200390017.

[7] J.O. Zoppe, N.C. Ataman, P. Mocny, J. Wang, J. Moraes, H.-A. Klok, Surface-Initiated Controlled Radical Polymerization: State-of-the-Art, Opportunities, and Challenges in Surface and Interface Engineering with Polymer Brushes, Chem. Rev. 117 (2017) 1105–1318. https://doi.org/10.1021/acs.chemrev.6b00314.

[8] W. Ma, S.K. Samal, Z. Liu, R. Xiong, S.C. De Smedt, B. Bhushan, Q. Zhang, C. Huang, Dual pH- and ammonia-vapor-responsive electrospun nanofibrous membranes for oil-water separations, J. Memb. Sci. 537 (2017) 128–139. https://doi.org/10.1016/j.memsci.2017.04.063.

[9] J. Borges, J.A. Ribeiro, E.M. Pereira, C.A. Carreira, C.M. Pereira, F. Silva, Preparation and characterization of DNA films using oleylamine modified Au surfaces, J. Colloid Interface Sci. 358 (2011) 626–634. https://doi.org/10.1016/j.jcis.2011.03.039.

[10] J.A. Jaber, J.B. Schlenoff, Recent developments in the properties and applications of polyelectrolyte multilayers, Curr. Opin. Colloid Interface Sci. 11 (2006) 324–329. https://doi.org/10.1016/j.cocis.2006.09.008.

[11] J.J. Richardson, M. Bjornmalm, F. Caruso, Technology-driven layer-by-layer assembly of nanofilms, Science. 348 (2015) aaa2491–aaa2491. https://doi.org/10.1126/science.aaa2491.

[12] J. Borges, J.F. Mano, Molecular Interactions Driving the Layer-by-Layer Assembly of Multilayers, Chem. Rev. 114 (2014) 8883–8942. https://doi.org/10.1021/cr400531v.

[13] Z. Zhang, S. Maji, A.B.D.F. Antunes, R. De Rycke, Q. Zhang, R. Hoogenboom, B.G. De Geest, Salt Plays a Pivotal Role in the Temperature-Responsive Aggregation and Layer-by-Layer Assembly of Polymer-Decorated Gold Nanoparticles, Chem. Mater. 25 (2013) 4297–4303. https://doi.org/10.1021/cm402414u.

[14] M. Safouane, R. Miller, H. Möhwald, Surface viscoelastic properties of floating polyelectrolyte multilayers films: A capillary wave study, J. Colloid Interface Sci. 292 (2005) 86–92. https://doi.org/10.1016/j.jcis.2005.05.061.

[15] A.M. Lehaf, H.H. Hariri, J.B. Schlenoff, Homogeneity, Modulus, and Viscoelasticity of Polyelectrolyte Multilayers by Nanoindentation: Refining the Buildup Mechanism, Langmuir. 28 (2012) 6348–6355. https://doi.org/10.1021/la300482x.

[16] M. Schönhoff, V. Ball, A.R. Bausch, C. Dejugnat, N. Delorme, K. Glinel, R. v. Klitzing, R. Steitz, Hydration and internal properties of polyelectrolyte multilayers, Colloids Surfaces A Physicochem. Eng. Asp. 303 (2007) 14–29. https://doi.org/10.1016/j.colsurfa.2007.02.054.

[17] M.F. Durstock, M.F. Rubner, Dielectric Properties of Polyelectrolyte Multilayers, Langmuir. 17 (2001) 7865–7872. https://doi.org/10.1021/la010954i.

[18] M.D. Miller, M.L. Bruening, Correlation of the Swelling and Permeability of Polyelectrolyte Multilayer Films, Chem. Mater. 17 (2005) 5375–5381. https://doi.org/10.1021/cm0512225.

[19] N. Zhao, F. Shi, Z. Wang, X. Zhang, Combining layer-by-layer assembly with electrodeposition of silver aggregates for fabricating superhydrophobic surfaces, Langmuir. 21 (2005) 4713–4716. https://doi.org/10.1021/la0469194.

[20] L. Zhai, F.C. Cebeci, R.E. Cohen, M.F. Rubner, Stable superhydrophobic coatings from polyelectrolyte multilayers, Nano Lett. 4 (2004) 1349–1353. https://doi.org/10.1021/nl049463j.

[21] J.D. Delgado, R.L. Surmaitis, S. Abou Shaheen, J.B. Schlenoff, Engineering Thiolated Surfaces with Polyelectrolyte Multilayers, ACS Appl. Mater. Interfaces. 11 (2019) 3524–3535. https://doi.org/10.1021/acsami.8b15514.

[22] X. Huang, J.D. Chrisman, N.S. Zacharia, Omniphobic Slippery Coatings Based on Lubricant-Infused Porous Polyelectrolyte Multilayers, ACS Macro Lett. 2 (2013) 826–829. https://doi.org/10.1021/mz400387w.

[23] S. Bai, C. Sun, H. Yan, X. Sun, H. Zhang, L. Luo, X. Lei, P. Wan, X. Chen, Healable, Transparent, Room-Temperature Electronic Sensors Based on Carbon Nanotube Network-Coated Polyelectrolyte Multilayers, Small. 11 (2015) 5807–5813. https://doi.org/10.1002/smll.201502169.

[24] Y. Li, F. Liu, J. Sun, A facile layer-by-layer deposition process for the fabrication of highly transparent superhydrophobic coatings, Chem. Commun. (2009) 2730. https://doi.org/10.1039/b900804g.

[25] E. Leguen, A. Chassepot, G. Decher, P. Schaaf, J.-C. Voegel, N. Jessel, Bioactive coatings based on polyelectrolyte multilayer architectures functionalized by embedded proteins, peptides or drugs, Biomol. Eng. 24 (2007) 33–41. https://doi.org/10.1016/j.bioeng.2006.05.023.

[26] C.D. Easton, A.J. Bullock, G. Gigliobianco, S.L. McArthur, S. MacNeil, Application of layer-by-layer coatings to tissue scaffolds – development of an angiogenic biomaterial, J. Mater. Chem. B. 2 (2014) 5558–5568. https://doi.org/10.1039/C4TB00448E.

[27] Y.-Z. Chang, J.-T. Lin, A. Prasannan, P.-C. Chen, C.-Y. Ko, H.-C. Tsai, Evaluation of the bacterial anti-adhesive properties of polyacrylic acid, chitosan and heparin-modified medical grade Silicone rubber substrate, J. Polym. Res. 22 (2015) 131. https://doi.org/10.1007/s10965-015-0767-6.

[28] M.H. Dufresne, J.C. Leroux, Study of the Micellization Behavior of Different Order Amino Block Copolymers with Heparin, Pharm. Res. 21 (2004) 160–169. https://doi.org/10.1023/B:PHAM.0000012164.60867.c6.

[29] T. Jiang, S. Zajforoushan Moghaddam, E. Thormann, PPEGMEMA-based cationic copolymers designed for layer-by-layer assembly, RSC Adv. 9 (2019) 26915–26926. https://doi.org/10.1039/C9RA05464B.

[30] F. Zhang, K. Sautter, A.M. Larsen, D.A. Findley, R.C. Davis, H. Samha, M.R. Linford, Chemical vapor deposition of three aminosilanes on silicon dioxide: Surface characterization, stability, effects of silane concentration, and cyanine dye adsorption, Langmuir. 26 (2010) 14648–14654. https://doi.org/10.1021/la102447y.

[31] T. Jiang, S.Z. Moghaddam, E. Thormann, A single-component, cross-linked, and surface-grafted polyelectrolyte film fabricated by the layer-by-layer assembly method, Polymer. 200 (2020) 122524. https://doi.org/10.1016/j.polymer.2020.122524.

[32] J. Rickert, A. Brecht, W. Göpel, QCM Operation in Liquids: Constant Sensitivity during Formation of Extended Protein Multilayers by Affinity., Anal. Chem. 69 (1997) 1441–8. https://doi.org/10.1021/ac960875p.

[33] M. V. Voinova, M. Rodahl, M. Jonson, B. Kasemo, Viscoelastic Acoustic Response of Layered Polymer Films at Fluid-Solid Interfaces: Continuum Mechanics Approach, Phys. Scr. 59 (1999) 391–396. https://doi.org/10.1238/Physica.Regular.059a00391.

[34] J.A. Woollam, B.D. Johs, C.M. Herzinger, J.N. Hilfiker, R.A. Synowicki, C.L. Bungay, Overview of variable-angle spectroscopic ellipsometry (VASE): I. Basic theory and typical applications, Proc. SPIE. 10294 (1999) 1029402. https://doi.org/10.1117/12.351660.

[35] J.J.I. Ramos, S.E. Moya, Water content of hydrated polymer brushes measured by an in situ combination of a quartz crystal microbalance with dissipation monitoring and spectroscopic ellipsometry, Macromol. Rapid Commun. 32 (2011) 1972–1978. https://doi.org/10.1002/marc.201100455.

[36] J.J. Iturri Ramos, S. Stahl, R.P. Richter, S.E. Moya, Water content and buildup of poly(diallyldimethylammonium chloride)/poly(sodium 4-styrenesulfonate) and poly(allylamine hydrochloride)/poly(sodium 4-styrenesulfonate) polyelectrolyte multilayers studied by an in situ combination of a quartz crystal microb, Macromolecules. 43 (2010) 9063–9070. https://doi.org/10.1021/ma1015984.

[37] D.E. Aspnes, J.B. Theeten, F. Hottier, Investigation of effective-medium models of microscopic surface roughness by spectroscopic ellipsometry, Phys. Rev. B. 20 (1979) 3292–3302. https://doi.org/10.1103/PhysRevB.20.3292.

[38] I. Reviakine, D. Johannsmann, R.P. Richter, Hearing what you cannot see and visualizing what you hear: Interpreting quartz crystal microbalance data from solvated interfaces, Anal. Chem. 83 (2011) 8838–8848. https://doi.org/10.1021/ac201778h.

[39] I. Choi, R. Suntivich, F.A. Plamper, C. V. Synatschke, A.H.E. Müller, V. V. Tsukruk, PH-controlled exponential and linear growing modes of layer-by-layer assemblies of star polyelectrolytes, J. Am. Chem. Soc. 133 (2011) 9592–9606. https://doi.org/10.1021/ja203106c.

[40] D. Chen, M. Wu, B. Li, K. Ren, Z. Cheng, J. Ji, Y. Li, J. Sun, Layer-by-Layer-Assembled Healable Antifouling Films, Adv. Mater. 27 (2015) 5882–5888. https://doi.org/10.1002/adma.201501726.

[41] C. Picart, J. Mutterer, L. Richert, Y. Luo, G.D. Prestwich, P. Schaaf, J.-C. Voegel, P. Lavalle, Molecular basis for the explanation of the exponential growth of polyelectrolyte multilayers, Proc. Natl. Acad. Sci. 99 (2002) 12531–12535. https://doi.org/10.1073/pnas.202486099.

[42] J.. Pieper, T. Hafmans, J.. Veerkamp, T.. van Kuppevelt, Development of tailor-made collagen–glycosaminoglycan matrices: EDC/NHS crosslinking, and ultrastructural aspects, Biomaterials. 21 (2000) 581–593. https://doi.org/10.1016/S0142-9612(99)00222-7.

[43] M. Zhang, X.H. Li, Y.D. Gong, N.M. Zhao, X.F. Zhang, Properties and biocompatibility of chitosan films modified by blending with PEG, Biomaterials. 23 (2002) 2641–2648. https://doi.org/10.1016/S0142-9612(01)00403-3.

[44] X. Chen, Y. Su, F. Shen, Y. Wan, Antifouling ultrafiltration membranes made from PAN-b-PEG copolymers: Effect of copolymer composition and PEG chain length, J. Memb. Sci. 384 (2011) 44–51. https://doi.org/10.1016/j.memsci.2011.09.002.